5

Structure and Deformation of Ice

"The pursuit of knowledge, brother, is the askin' of many questions."
Raymond Chandler, *Farewell my Lovely*

INTRODUCTION

Fundamental to all theoretical treatments of glacier flow, and of deformation in other materials, is the so-called *constitutive relation*, a formula relating the amount and rate of deformation to the applied stress. This is a property of the material and has to found by experiment. In an elastic material, for example, deformation and stress are proportional, whereas in a Newtonian viscous material, the *rate* of deformation is proportional to the stress. In a perfectly plastic material, a gradually increasing stress produces no deformation until a critical value, the yield stress, is reached, when rapid deformation begins.

In glacier studies, the constitutive relation is usually called the *flow law of ice*. This is misleading; it is not a universal "law". The relation depends on the loading conditions, confining pressure, state of stress, and other factors. For example, ice responds elastically to high-frequency sound waves; this is the basis of the seismic method of measuring ice thickness. On the other hand, ice may fracture if a large stress is applied rapidly. If the stress is applied slowly, as in glacier flow, the ice becomes permanently deformed in a way that is intermediate between Newtonian viscous and perfectly plastic behaviour.

As a preliminary to discussing ice deformation, I briefly describe the structure of the ice crystal. The results of mechanical tests on ice in the laboratory are then described. These have established how the deformation rate depends on stress and temperature. Impurities and the

orientation of the crystals also influence the deformation rate, however, and these observations are difficult to quantify. In addition to quoting experimental results, I briefly describe the deformation mechanisms. Simple stress systems such as uniaxial compression are used in laboratory tests whereas stress systems in glaciers are complex. The flow relation has to be generalized to cover such cases. Appropriate values of the parameters in the flow relation, obtained from both field and laboratory data, are then given.

The concepts of stress and strain, which are fundamental to the understanding of this chapter, are outlined in Appendix 1.

STRUCTURE OF THE ICE CRYSTAL

First we consider the structure of a molecule of H_2O. The three nuclei of this molecule can be pictured as forming an isosceles triangle with the oxygen nucleus at the apex and the hydrogen nuclei (protons) at the other two corners. The oxygen atom has eight electrons, two of which circle close to the nucleus. Another two rotate in eccentric orbits each of which also contains the electron from one of the hydrogen atoms. Each of these orbits thus encloses the oxygen nucleus and one proton. The remaining four electrons rotate in two other eccentric orbits. The four eccentric orbits radiate tetrahedrally from the oxygen nucleus. The electron orbits completely screen the oxygen nucleus. They do not screen all the positive charge of the protons, however, and they also provide an excess negative charge in the directions of the two orbits without protons. We can thus picture the ice molecule as a regular tetrahedron with positive charges in two corners and negative charges in the other two. Moreover, each negative corner attracts a positive corner in a neighbouring molecule, joining the molecules together by a *hydrogen bond.* Thus each molecule is surrounded by four other molecules in a regular tetrahedral arrangement. The spacing between molecules in ice is 0.276 nm.

A substance in which every atom has four neighbours in regular tetrahedral arrangement can crystallize hexagonally or cubically. Studies of ordinary ice by X-ray diffraction have shown that the molecules, or rather, the oxygen atoms are arranged in layers of hexagonal rings. The atoms in a ring are not in one plane but in two, however: alternate atoms are in the upper and lower planes. The spacing between these two planes is much less than the spacing between the layers. Adjacent layers are mirror images of each other. Figure 5.1 shows this arrangement and its relation to the tetrahedral structure. The structure of the ice crystal resembles that of a hexagonal metal such as magnesium or cadmium. The plane

of a layer of hexagonal rings is called the *basal plane* of the crystal. The direction at right angles to the basal plane is the *optic axis* or *c-axis.*

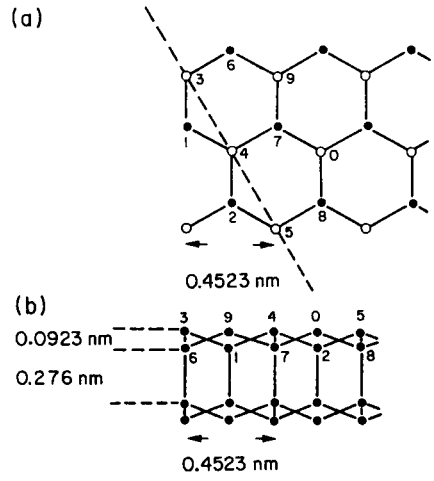

FIG. 5.1. Structure of ice crystal. The circles denote oxygen atoms. The numbers denote corresponding atoms in the two diagrams. (a) Projection of lattice on basal plane. Light and dark circles denote atoms in two planes 0.0923 nm apart: the bonds between atoms are thus oblique to the plane of the paper. (b) Projection of lattice on plane containing the *c*-axis and the broken line in (a). The atoms shown are in four different planes (12), (345), (678), (90).

DEFORMATION OF A SINGLE ICE CRYSTAL

How an ice crystal deforms under an applied stress has been studied extensively in the laboratory. The usual method is to apply a constant stress, with the crystal oriented so that there is a component of shear stress in its basal plane, and measure how the deformation (strain) changes with time. When the stress is first applied, the ice immediately deforms elastically by a certain amount; permanent deformation (*creep*) then begins and continues as long as the stress is applied. Two important features are: (1) Even very low stresses cause deformation and (2) the deformation takes place in discrete bands, parallel to the basal planes of the crystal. These bands can be seen clearly in polarized light. A single ice crystal

normally deforms by gliding on its basal planes. The crystal resembles a pack of cards with the faces representing the basal planes; the pack is easily deformed if the cards can slide over each other. Although crystals unfavourably oriented for basal glide can still deform, the stress needed to produce a given deformation is about 100 times that for basal glide and the stress-strain curve has a different shape (Muguruma and others, 1966).

The deformation of ice and metals can be understood in terms of the movement of *dislocations* within the crystals (Weertman and Weertman, 1964). A dislocation is a linear defect in the crystal structure; it can be regarded as the boundary between two regions, one of which has slipped relative to the other. Dislocations allow planes of atoms to move past each other much more easily than they would in a perfect crystal. This explains why even a low stress produces some deformation. Deformation involves the movement of dislocations within the crystal; it also produces additional dislocations. One dislocation may block the movement of others and so cause them to "pile up" at some points. These pile-ups resist further deformation and so harden the material. To soften it again, the dislocations have to be dispersed into some more nearly uniform arrangement. Several mechanisms can cause dislocations to move through a crystal and different materials have different preferred mechanisms. Ice deforms most readily by the movement of dislocations in the basal plane and there is apparently no preferred direction in that plane (Glen, 1975, p. 11).

DEFORMATION OF POLYCRYSTALLINE ICE

Figure 5.2a shows a typical *creep curve* (graph of strain versus time) obtained when a polycrystalline aggregate of ice, in which the orientation of the individual crystals is random, is subjected to a constant stress. An initial *elastic deformation AB* is followed by a period of *primary* or *transient creep* in which the strain rate decreases continuously until a minimum value, the *secondary creep* rate, is reached. The strain rate increases after that (*tertiary creep*) and, if the test is carried on for long enough, a steady value is eventually reached. A logarithmic plot of strain rate against strain or time (Fig. 5.2b) shows these features clearly.

If the initial orientation of the crystals is random, the minimum creep rate is attained when the total strain reaches about 1 per cent, irrespective of the stress and temperature (Jacka, 1984a). The minimum creep rate of a polycrystalline aggregate is less than one per cent of the steady creep rate of a single crystal, oriented for glide in its basal plane, at the same stress and temperature (Butkovich and Landauer, 1958). The tertiary

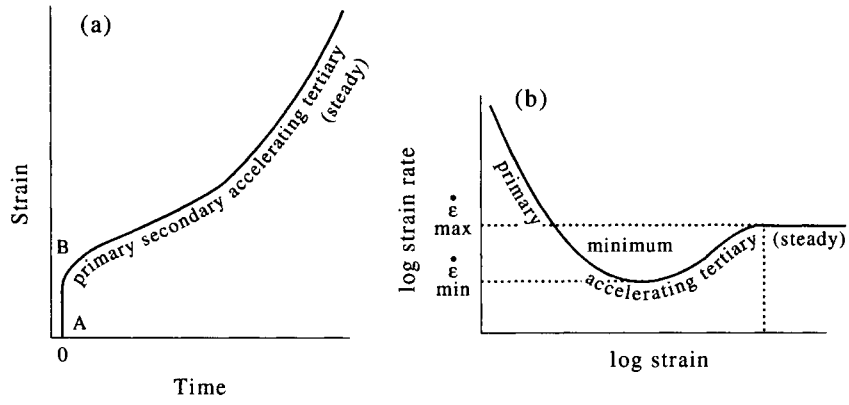

FIG. 5.2. (a) Typical creep curve (strain versus time) of polycrystalline ice, with random orientation of individual crystals, showing the different stages of creep. (b) Corresponding logarithmic plot of strain rate versus strain. Adapted from Budd and Jacka (1989) by permission of Elsevier Science Publishers.

creep rate may become steady after total compressive strains of 10 to 15 per cent (Jacka and Maccagnan, 1984). In compression, the steady tertiary creep rate is three or four times the minimum, whereas in shear the factor is about ten (Steinemann, 1958b, Budd and Jacka, 1989).

Several processes contribute to the deformation of polycrystalline ice. In addition to movement of dislocations within crystals, the crystals move relative to each other. Crystal growth, the migration of crystal boundaries, and *dynamic recrystallization* (the nucleation and growth of new crystals favourably oriented for deformation) are also important. Polycrystals deform much more slowly than a single crystal because most of the crystals are not oriented for basal glide in the direction of the applied stress. The hardening in transient creep results from interference between crystals with different orientations. Production, by recrystallization, of crystals more favourably oriented for glide in the direction of the stress, causes the increased strain rate in tertiary creep. Multiplication of dislocations and formation of microcracks may also contribute. The onset of tertiary creep does not necessarily coincide with the start of recrystallization. During secondary creep, the ice may be recrystallizing at those grain boundaries where stresses are particularly high; the observed minimum strain rate probably results from a temporary balance between

softening at those parts of the sample and hardening elsewhere. Thus secondary creep is not truly steady-state creep, although it is often referred to as such. Moreover, the development of favourably-oriented crystals continues even after a steady tertiary creep rate has been attained (Jacka and Maccagnan, 1984).

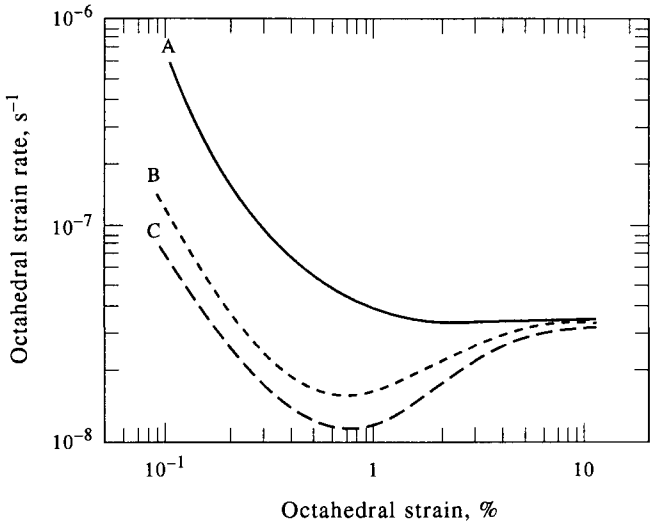

FIG. 5.3. Graphs of strain rate versus strain for three tests in unconfined uniaxial compression at 200 kPa and –3° C. Curve A: ice with an initial fabric (a small-circle girdle) that favoured compression. Curve B: ice with an initially random fabric. Curve C: ice with an initial fabric (a single maximum) unfavourable for compression. Note that the three samples reached the same final strain rate and they all developed a small-circle girdle fabric. From Jacka and Budd (1991) by permission of Springer-Verlag.

Deformation changes the average crystal size and an equilibrium size is approached as the tertiary creep rate becomes steady. (Jacka and Budd, 1991). The equilibrium size is independent of the initial size and depends mainly on the stress; the higher the stress, the smaller the crystal. This dependence arises because a high stress produces a high strain rate and therefore a high total strain and with increase of strain the rate of nucleation of new grains increases more rapidly than the crystal-growth rate

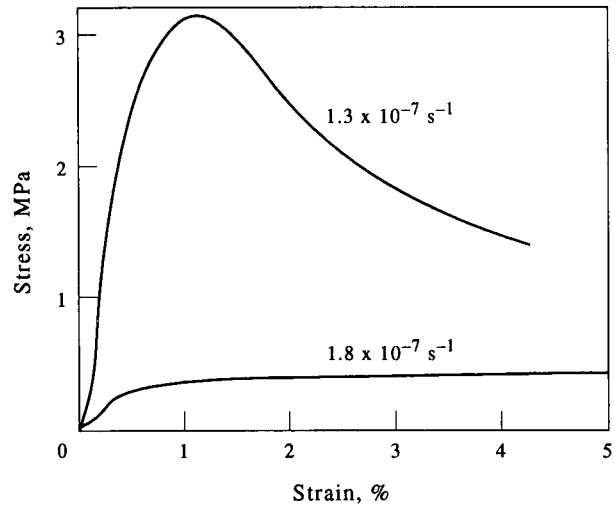

FIG. 5.4. Graphs of stress versus strain for tests at constant strain rate. Curve a: ice with an initial fabric unfavourable for deformation under the applied stress. Curve b: ice with a favourable initial fabric. From Shoji and Langway (1988). Adapted from *Annals of Glaciology* by permission of the International Glaciological Society.

(Glen, 1955). This effect must be important in glaciers because shear bands are characterized by small crystals. A similar inverse relation between recrystallized grain size and applied stress is found in certain minerals (Poirier, 1985, p. 185).

If the crystals in the sample are not randomly oriented at the start of the test, the shape of the creep curve depends on whether the applied stress configuration is compatible with the pre-existing crystal orientation fabric. If it is compatible, that is, if it is the same configuration as that which produced the fabric, the minimum strain rate is higher than that of a randomly oriented sample. Indeed, if the initial fabric is strong, the steady tertiary creep rate is attained as soon as the transient stage is completed. If the initial fabric is incompatible with the applied stress, the minimum strain rate is lower than that of a randomly-oriented sample at the same stress and temperature. Figure 5.3 illustrates these cases. The mechanisms of fabric formation are discussed in Chapter 9.

A test at constant strain rate is an alternative to one at constant

stress. Figure 5.4 shows typical creep curves for this case. For ice with an initially random fabric, or with a fabric incompatible with the applied stress, the stress attains a maximum after the initial transient stage. This corresponds to the minimum strain rate in a constant stress test. If on the other hand the ice has a fabric compatible with the applied stress, the curve shows "stress saturation", that is the stress becomes steady immediately after the transient stage.

FLOW RELATION FOR POLYCRYSTALLINE ICE

Form of Relation

Numerous laboratory experiments have shown that, for secondary creep of ice over the range of stresses important in normal glacier flow (50–200 kPa or 0.5–2 bars) the relation between the shear strain rate $\dot{\epsilon}_{xy}$ and the shear stress τ_{xy} has the form

$$\dot{\epsilon}_{xy} = A\tau_{xy}^{n}. \tag{1}$$

Here n is a constant but A depends on ice temperature, crystal orientation, impurity content and perhaps other factors. This is often called *Glen's Law.* Although the form of the relation is well-established and can be explained in terms of dislocation theory, it is essentially an empirical fit to laboratory and field data for the loading conditions and stresses encountered in glaciers. Different experimenters have obtained widely different values of A and n; measured strain rates for a given stress and temperature differ by a factor of about 10 (Weertman, 1973, Fig. 4). Values of n vary from 1.5 to 4.2 (Weertman, 1973, Table 2) with a mean of about 3, the value normally adopted in glacier studies. The flow of ice thus differs markedly from that of a viscous fluid for which $n = 1$ and $1/A$ is the viscosity.

The question whether n is a constant has been widely discussed. Barnes and others (1971) found that n increased with stress for stresses greater than about 500 kPa; however, shear stresses in glaciers never reach this value. Of more importance is the suggestion that, at stresses below about 100 kPa, n decreases to a value near 1 (*e.g.* Mellor and Smith, 1967; Mellor and Testa, 1969b). Weertman (1969b, 1973), however, argued that these experiments were not carried on long enough to reach the minimum strain rate. If the strain rates at low stresses are too high, the slope of the graph of $\log \dot{\epsilon}_{xy}$ versus $\log \tau_{xy}$, and thus the apparent value of n, is reduced. Russell-Head and Budd (1979) carried on low-stress tests for periods of up to two years in order to obtain minimum creep rates; their data give $n = 3$.

Most of the evidence for $n = 3$ comes from either laboratory tests or deformation measurements in temperate glaciers. Dynamic recrystallization occurs in all these cases. But it does not occur in ice sheets or ice caps when the temperature is below about −12°C. Pimienta and Duval (1987) have argued that in these circumstances n should be less than 3. Alley (1992) has discussed this. The only good field data, from Dye 3 in Greenland, are consistent with any value of n between 2 and 3 (Dahl-Jensen and Gundestrup, 1987). Until more data are available, it seems best to continue to use $n = 3$ in ice-sheet modelling.

Effect of Temperature

The value of A varies with temperature T according to the *Arrhenius relation*

$$A = A_0 \exp(-Q/RT), \tag{2}$$

where A_0 is independent of temperature, R is the universal gas constant ($8.314\,\mathrm{J\,mol^{-1}K^{-1}}$), and Q is the *activation energy for creep.* Results of laboratory experiments on polycrystalline ice at temperatures below −10°C give values of Q from 42 to 84 kJ/mol with a mean of 60 kJ/mol (Weertman, 1973, Table 2). This is apparently equal to the *activation energy for volume self-diffusion* (Weertman, 1973, Table 3), the process by which individual molecules of H_2O move through the ice lattice. This value implies that the strain rate produced by a given stress at −10°C is about 5 times that at −25°C. For glacier ice, Paterson (1977) obtained a value of 54 kJ/mol from measurements of closure rate of boreholes drilled in polar ice caps. At temperatures above −10°C, the value of Q for polycrystalline ice appears to increase to about 139 kJ/mol (mean of 4 values) (Weertman, 1973, Table 2). To explain this, Barnes and others (1971) suggested that grain-boundary sliding and the presence of liquid at grain boundaries contribute to creep in this temperature range. Jones and Brunet (1978) confirmed this by showing that the creep activation energy for single crystals does not increase near the melting point. Above −10°C, the effective value of Q for polycrystalline ice is not constant but increases with temperature (Mellor and Testa, 1969a, Fig. 3). In effect, the Arrhenius relation breaks down, as is expected when several creep processes are operating simultaneously. Current practice in theoretical analyses and computer modelling of glacier flow is to use the Arrhenius relation at all temperatures. Above −10°C, an empirical relation between strain rate and temperature, for fixed stress, might be preferable; if the Arrhenius relation is retained, the value of Q should be increased from 60 to 139 kJ/mol.

Activation energies are sometimes expressed in electron volts (1 eV = 1.6021×10^{-19} J). In this case, the exponential factor in Eq. 2 is written $\exp(-Q/kT)$ where k is Boltzmann's constant, which is the gas constant R divided by the Avogadro number N, the number of molecules in one mole. Because $N = 6.022 \times 10^{23}\,\mathrm{mol}^{-1}$, an activation energy of 60 kJ/mol corresponds to 0.62 eV.

Effect of Pressure

The value of A_0 in Eq. 2 depends on the hydrostatic pressure P. The relation is

$$A_0 = A_0' \exp(-PV/RT). \tag{3}$$

Here V is the *activation volume for creep.* Calculations and two preliminary experiments give a mean value of $-1.7 \times 10^4\,\mathrm{mm}^3/\mathrm{mol}$ (Weertman, 1973, Table 4). This pressure effect is very small even for the hydrostatic pressures that exist at the base of the Greenland and Antarctic Ice Sheets. It can be assumed, as Rigsby (1958) suggested, that hydrostatic pressure does not affect the flow relation provided that temperature is measured relative to the freezing point. Hydrostatic pressure does of course depress the freezing point. Further laboratory work is needed to confirm the sign and value of V.

The value of A_0 also depends on the orientation of the crystals and on the water content and concentration of impurities in the ice.

Effect of Crystal Size and Orientation

Laboratory tests at temperatures between −7 and −10°C , where the water content is negligible, have shown that the minimum (secondary) creep rate is independent of crystal size (Duval and LeGac, 1980; Jacka, 1984b). Jacka also explained why some previous investigators had found an apparent size-dependence. On the other hand, the transient creep rate increases with crystal size (Duval, 1973). As a result, coarse-grained ice reaches minimum creep rate more rapidly than fine-grained. (In ice, a grain is the same as a crystal.) Jacka (1984b) also found that the steady tertiary creep rate was independent of the initial crystal size. I discuss the dependence of A_0 on crystal orientation in the section about anisotropic ice.

Effect of Water

Duval (1977) studied this by performing mechanical tests on ice samples from a temperate glacier. The data could be fitted by a linear relation

$$A_0 = (3.2 + 5.8\,W) \times 10^{-15}\,(\mathrm{kPa})^{-3}\,\mathrm{s}^{-1}, \tag{4}$$

where W is the percentage water content and A_0 refers to tertiary creep (Lliboutry and Duval, 1985). The average value of W in the basal layers, the most important ones in glacier flow, was 0.33 per cent. Water enhances the deformation rate of polycrystalline ice by facilitating the adjustment between neighbouring grains with different orientations, an adjustment that occurs by both grain-boundary sliding and by melting and refreezing (Barnes and others, 1971).

Effect of Impurities

How solid inclusions change the creep rate of ice is unclear and more data are needed. Nayar and others (1971) deformed ice containing dispersed particles of silica and obtained secondary creep rates of only 0.03 to 0.1 times those in pure ice at the same stress and temperature. The average particle size was 0.015 μm and the concentration 1 per cent by volume. Hooke and others (1972) found that the creep rate of ice containing sand decreased exponentially with increase of sand concentration above 10 per cent. Tests at lower concentrations gave no consistent results. Swinzow (1962) studied ice bands in a tunnel at the margin of the Greenland Ice Sheet. Bands with evely-dispersed fine silt, with few contacts between particles, deformed more readily than clean ice. Bands containing silt and rock with many particles touching each other were stiffer than clean ice.

Soluble impurities usually increase the creep rate. Dissolved impurities may be found at different places in ice. A few molecules (HF, NH_3 and, at low concentrations, HCl) dissolve *substitutionally*, that is, they replace an H_2O molecule in the crystal structure. Because the structure is relatively open, small molecules can also fit into the holes (*interstitial* impurity); HCl, but not H_2SO_4, can do this. Impurities may also be at the grain boundaries and, if the temperature is above the eutectic temperature, they form a liquid layer. Mulvaney and others (1988), for example, detected sulphuric acid at three-grain junctions in Antarctic ice.

Laboratory tests have shown that HF and HCl, at concentrations of a few parts per million, increase the deformation rate of single crystals of ice by a factor of at least 10 (Jones and Glen, 1969; Nakamura and Jones, 1970). The impurities, dissolved substitutionally, create additional point defects in the crystal structure and these increase the speed of reorientation of those hydrogen bonds that are obstructing the movement of dislocations. Interstitial impurities probably do not change the deformation rate.

For polycrystalline ice, Raraty and Tabor (1958) found that, in the temperature range 0 to –25°C , ice containing 1 per cent of "Teepol"

(sodium dodecyl sulphate) had a creep rate 5 times that of pure ice; below −25°C the creep rates were the same. They suggested that −25°C was the eutectic temperature of the system. Above this temperature, some unfrozen Teepol-rich solution existed between the ice crystals and softened the ice by facilitating adjustments between grains; below −25°C the system behaved like pure ice. Sodium chloride (eutectic temperature −21°C) from the ocean and sulphuric and hydrochloric acid (−73°C, −75°C) from volcanoes are sometimes found at sufficiently high concentrations to influence the flow of polar ice sheets. I discuss this later in the chapter.

Effect of Density

Figure 5.5 shows the variation of minimum strain rate with density. These results are consistent with the data in an earlier compilation by Mellor (1975, Fig. 16). Above the pore close-off density, there is no significant variation in strain rate. This implies that air bubbles have no effect on the mechanical properties of ice. In firn, however, the strain rate increases by a factor of about 10 per $150\,\mathrm{kg\,m^{-3}}$ decrease in density. Densification accounts for some of the increased strain in firn relative to that in ice. Because a significant part of some polar ice masses, ice caps in arctic Canada and some Antarctic ice shelves for example, consist of firn, its mechanical properties may be important for their dynamics. However, because firn is compressible whereas ice is not, its constitutive relations are complex.

THE GENERALIZED FLOW RELATION

The Relation

In most laboratory tests, uniaxial compression, or simple shear is used. Stress systems in glaciers are complex and so the simple flow relation (Eq. 1) has to be generalized. Nye (1957) discussed how to do this. The ice is assumed to be homogeneous, isotropic and incompressible. The isotropic assumption means that the relation applies to secondary but not tertiary creep.

Normal-stress components are denoted by σ_x, σ_y, σ_z, shear-stress components by τ_{xy}, τ_{yz}, τ_{zx}, and strain-rate components by $\dot{\epsilon}_x$, $\dot{\epsilon}_y$, $\dot{\epsilon}_z$, $\dot{\epsilon}_{xy}$, $\dot{\epsilon}_{yz}$, $\dot{\epsilon}_{zx}$. Experiments show that, to a good approximation, the flow relation is unaffected by hydrostatic pressure. The best way to express this is to work with *stress deviators* rather than stresses. The stress-deviator components are obtained by subtracting the amplitude of the hydrostatic pressure (the mean normal stress) from each normal-stress component. Thus

$$s_x = \sigma_x - \tfrac{1}{3}(\sigma_x + \sigma_y + \sigma_z) \tag{5}$$

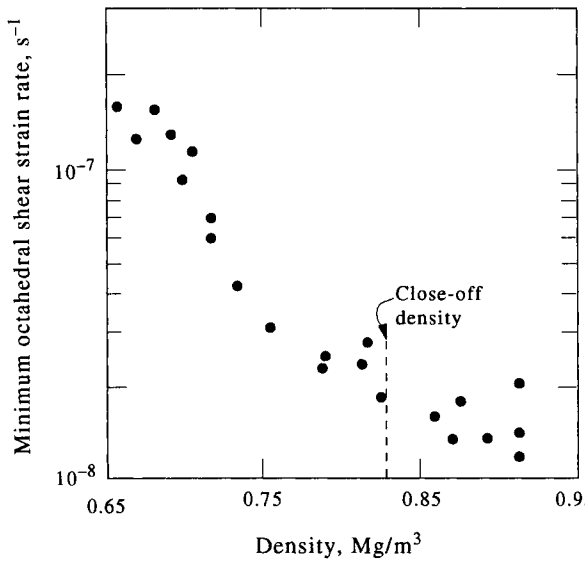

FIG. 5.5. Variation of minimum octahedral shear strain rate with initial density. The tests were in unconfined, uniaxial compression with an octahedral shear stress of 200 kPa, at −3° C. From Hooke and others (1988). Reproduced from the *Journal of Glaciology* by permission of the International Glaciological Society.

and similarly for s_y, s_z. The shear-stress components are unchanged. It follows that

$$s_x + s_y + s_z = 0. \tag{6}$$

It is the stress deviators, not the stresses, that cause deformation in an incompressible material.

A flow relation for complex stress systems must connect quantities that describe the overall state of stress and strain rate. Moreover, it is a physical property of the material and cannot be affected by the way in which the coordinate axes are drawn.

To proceed further, two assumptions are made.

1. At any point, each strain-rate component is proportional to the corresponding stress-deviator component. This is a reasonable assumption for an isotropic material. Thus

$$\dot{\epsilon}_x = F s_x \; ; \qquad \dot{\epsilon}_{xy} = F \tau_{xy} \tag{7}$$

and similar relations. The factor F is a function of position. It follows from Eq. 6 that

$$\dot{\epsilon}_x + \dot{\epsilon}_y + \dot{\epsilon}_z = 0, \tag{8}$$

which is consistent with the assumption that ice is incompressible.

2. Nye, following Odqvist (1934; 1966, p. 21), proposed using the quantities $\dot{\epsilon}$, τ, called the *effective strain rate* and *effective shear stress* or *effective deviator stress*, defined by

$$2\dot{\epsilon}^2 = \dot{\epsilon}_x^2 + \dot{\epsilon}_y^2 + \dot{\epsilon}_z^2 + 2(\dot{\epsilon}_{xy}^2 + \dot{\epsilon}_{yz}^2 + \dot{\epsilon}_{zx}^2) \tag{9}$$

$$2\tau^2 = s_x^2 + s_y^2 + s_z^2 + 2(\tau_{xy}^2 + \tau_{yz}^2 + \tau_{zx}^2), \tag{10}$$

where $\dot{\epsilon}$ and τ are always taken to be positive. (The *octahedral* strain rate and shear stress are sometimes used instead. The relations are $3\dot{\epsilon}_{\text{oct}}^2 = 2\dot{\epsilon}^2$, $3\tau_{\text{oct}}^2 = 2\tau^2$.) The flow relation is assumed to be a relation between $\dot{\epsilon}$ and τ, specifically

$$\dot{\epsilon} = A\tau^n, \tag{11}$$

where A and n have the values determined for randomly-oriented polycrystals in simple shear. It can be shown that values of $\dot{\epsilon}$ and τ are not changed by any rotation of the coordinate axes (Jaeger, 1962, p. 14). Equation 11 reduces to Eq. 1 when $\dot{\epsilon}_{xy}$ and τ_{xy} are the only non-zero components. The generalized relation is therefore consistent with the simple one. From Eqs. 7, 9 and 10 it follows that

$$\dot{\epsilon} = F\tau \tag{12}$$

and by Eq. 11

$$F = A\tau^{n-1}. \tag{13}$$

Thus, by Eq. 7, the relations between strain-rate and stress-deviator components are

$$\dot{\epsilon}_x = A\tau^{n-1}s_x \; ; \qquad \dot{\epsilon}_{xy} = A\tau^{n-1}\tau_{xy}. \tag{14}$$

Readers familiar with tensors will recognize that $2\dot{\epsilon}^2$ and $2\tau^2$ are the second invariants of the strain-rate and stress-deviator tensors. The most general relation between two such tensors involves their first, second and third invariants. The first invariants are the left-hand sides of Eqs. 6 and 8. The third invariants are the determinants of each tensor or, equivalently, the product of the three principal strain rates or principal stress deviators.

When the first invariants are zero, as here, the general relation reduces to (Glen, 1958)

$$\dot{\epsilon}_{ij} = B(I_2, I_3)s_{ij} + C(I_2, I_3)(s_{ik}s_{kj} - \tfrac{2}{3}I_2\delta_{ij}). \tag{15}$$

Here B and C are functions of I_2 and I_3, the invariants of the stress deviator tensor, δ_{ij} is the Kronecker delta, and repeated suffixes imply summation. Nye's two assumptions reduce this equation to $\dot{\epsilon}_{ij} = B(I_2)s_{ij}$. In a two-dimensional analysis ("plane strain"), which is often used in glacier mechanics, the second assumption is unnecessary because $I_3 = 0$; but the first one must still be made.

Test of Assumptions

To test the validity of Nye's assumptions, ice must be subjected to a combination of stresses, simultaneous shear and compression for example. Baker (1987) made such tests and summarized previous work. He concluded, contrary to the results of three of the four previous tests, that neither assumption was strictly valid. However, the size of the deviations relative to the precision of the measurements is unclear. The question needs further study. Failure of the assumptions would imply, for example, that a sample in simple shear would expand or contract in the direction perpendicular to the shear plane and, because ice is incompressible, this would be accompanied by contraction or expansion in the shear plane. Thus, if the assumptions fail and Eq. 15 has to be used instead of Eq. 14, not only does analysis become much more complicated but plane-strain models could no longer be used.

Special Cases of Equation 11

1. Simple shear

$$\dot{\epsilon}_{xz} = A\tau_{xz}^3. \tag{16}$$

This stress system applies near the base of a glacier.

2. Unconfined uniaxial compression in the vertical (z) direction.

$$\begin{aligned} &\sigma_x = \sigma_y = 0 \\ &s_z = \tfrac{2}{3}\sigma_z\ ; \qquad s_x = s_y = -\tfrac{1}{3}\sigma_z \\ &\dot{\epsilon}_x = \dot{\epsilon}_y = -\tfrac{1}{2}\dot{\epsilon}_z \\ &\dot{\epsilon}_z = \tfrac{2}{9}A\sigma_z^3. \end{aligned} \tag{17}$$

This stress system applies in most laboratory experiments and in the near-surface layers of an ice sheet. Comparison of Eqs. 16 and 17 shows that the

strain rate produced by a given compression (or tension) is only two ninths of that produced by an equal shear stress. Some laboratory tests suggest that the difference may be even larger than this (Budd and Jacka, 1989, Fig. 5).

3. Uniaxial compression, confined in the y-direction.

$$\begin{aligned} &\sigma_x = 0\ ; \qquad \dot{\epsilon}_y = 0\ ; \qquad \dot{\epsilon}_x = -\dot{\epsilon}_z \\ &s_y = \tfrac{1}{3}(2\sigma_y - \sigma_z) = 0\ ; \qquad \sigma_y = \tfrac{1}{2}\sigma_z \\ &s_x = -s_z = -\tfrac{1}{3}(\sigma_y + \sigma_z) = -\tfrac{1}{2}\sigma_z \\ &\dot{\epsilon}_z = \tfrac{1}{8}A\sigma_z^3. \end{aligned} \tag{18}$$

A non-zero σ_y is required to prevent extension in the y-direction. This stress system applies in the near-surface layers of a valley glacier and in an ice shelf occupying a bay.

4. Shear combined with unconfined uniaxial compression

$$\sigma_x = \sigma_y = \tau_{xy} = \tau_{yz} = 0$$

$$s_z = \tfrac{2}{3}\sigma_z = -2s_x = -2s_y$$

$$\tau^2 = \tfrac{1}{3}\sigma_z^2 + \tau_{xz}^2 \tag{19}$$

$$\dot{\epsilon}_z = -2\dot{\epsilon}_x = -2\dot{\epsilon}_y = \tfrac{2}{3}\tau^2\sigma_z \tag{20}$$

$$\dot{\epsilon}_{xz} = A\tau^2\tau_{xz}. \tag{21}$$

This stress configuration applies at many places in ice sheets.

Implications of Non-linear Flow Relation

As Eq. 14 with $n = 3$ shows, each strain-rate component is proportional, not only to the corresponding stress deviator, but also to the square of the effective shear stress. This increases with each stress deviator. Thus an individual stress component acting by itself produces a smaller strain rate than it would in the presence of other stresses. For example, a tunnel dug in a glacier closes up under the pressure of the ice above it. At the foot of an icefall there is a large longitudinal compressive stress in the ice. Thus a tunnel there should close up much more rapidly than it would at the same depth in a part of the glacier where other stress components are small. This has been confirmed on Austerdalsbre in Norway (Glen, 1958). Again, the flow of ice under its own weight tends to eliminate crevasses, waves or large hummocks on the glacier surface. This should happen more rapidly at the foot of an icefall than elsewhere.

Furthermore, the presence of additional stress components may effectively change the form of the relation between a strain-rate component and its corresponding stress deviator. For example, if τ_{xy} is the only non-zero stress-deviator component, $\tau = \tau_{xy}$ and Eq. 4, with $n = 3$, shows that $\dot{\epsilon}_{xy}$ varies as τ_{xy}^3. However, if there is a longitudinal stress-deviator component s_x which is large compared with τ_{xy}, τ will be approximately equal to s_x and $\dot{\epsilon}_{xy}$ will be proportional to $s_x^2\tau_{xy}$. Thus, $\dot{\epsilon}_{xy}$ now varies linearly with τ_{xy}. This illustrates the complicated effects of a non-linear flow law and emphasizes the necessity of taking all stress components into account when trying to determine the value of n from measurements of deformation in a glacier. Several published analyses have failed to do this.

The flow relation is sometimes written in the inverse form

$$s_x = \eta\dot{\epsilon}_x \; ; \qquad \tau_{xy} = \eta\dot{\epsilon}_{xy}, \tag{22}$$

where η is an *effective viscosity.* Unlike the case of hydrodynamics, however, where viscosity is a constant because the flow relation is linear, η varies with the stress.

FIELD MEASUREMENTS OF FLOW PARAMETERS

In glaciers and ice sheets, the deep ice is deformed for hundreds or thousands of years to total strains of perhaps ten or more. Many laboratory tests determine the flow parameters only for secondary creep at total strains of a few per cent. To obtain results in periods of weeks rather than years, stresses and sometimes temperatures higher than those in an ice sheet are used. This may change conditions and possibly introduce different deformation mechanisms such as dynamic recrystallization. (See Chapter 9.) Even with increased stress and temperature it is sometimes difficult to carry on tests for long enough to ensure that a minimum creep rate, let alone a steady tertiary one, has been reached.

Field measurements of flow parameters are therefore desirable. They are of three types: (1) measurement of the rate at which an initially-vertical borehole tilts as a result of shear within the glacier (*e.g.* Nye, 1957), (2) measurement of the rate at which a floating ice shelf spreads under its own weight (Thomas, 1973b) and (3) measurement of the rate at which tunnels and boreholes in glaciers close as a result of the pressure of the overlying ice (Nye, 1953; Paterson, 1977). A disadvantage of all field experiments is that stresses cannot be measured; they have to be calculated on the basis of some simplified model. Moreover, each type of

experiment has additional drawbacks. Measurements of borehole tilt are difficult to interpret because the glacier is not usually deforming in simple shear; there are also longitudinal stresses. As explained in the previous section, failure to take these into account can change the apparent value of n. Temperatures in floating ice shelves range from roughly –20°C at the surface to the freezing point of sea water (–1.8°C) at the base. Thus measurements of spreading rate give a value of the parameter A averaged over this temperature range. Borehole closure does not measure steady ice deformation. Moreover, because total strain decreases with increasing distance from the hole wall, transient, secondary, and tertiary creep may be occurring simultaneously in different parts of the ice; only the resultant creep rate at the hole wall can be measured. The data are analyzed by drawing creep curves and interpreting the minimum creep rate as secondary creep.

In addition, the value of A_0 (Eq. 2) tends to increase with depth as the ice develops a preferred crystal orientation. In this case, a graph of strain rate against stress on logarithmic scales is not a straight line and the slope of a straight line fitted to the data gives too high a value of n. This might explain the high values observed in some borehole-tilt experiments, for example $n = 13$ for ice near the base of Blue Glacier (Kamb and Shreve, 1966). In fact, A_0 can vary significantly over short vertical distances as Figs. 11.16 and 11.17 show. In this case, a depth-averaged value derived from field measurements is more useful for modelling purposes than spot values obtained from laboratory tests on a few core samples about 100 mm long.

VALUES OF FLOW PARAMETER A

As described above, experimental data suggest that over the range of stresses important in glacier flow, the index n in the flow relation is about 3 and the creep activation energy Q is about 60 kJ/mol below –10°C and has a mean value of about 139 kJ/mol at temperatures between –10°C and 0°C . In what follows I adopt these values and then derive values of the multiplier A (Eqs. 1 and 11) that fit the data. Some authors use a value of n other than 3. In these cases I calculated A for $n = 3$ from their measured strain rate at an effective shear stress of 100 kPa.

Table 5.1 summarizes the data at three temperatures. In view of the large amount of data at the melting point, I quote only the results of compilations. Although the water content influences the value of A, it was not measured. I chose –2°C as the lowest temperature at which the effect of any water in the ice is significant. The data quoted are from tests

at this temperature. The data for −10°C are from experiments at this temperature and below, converted to −10°C using an activation energy of 60 kJ/mol. The data of Shoji and Langway and of Dahl-Jensen and Gundestrup refers to ice from the borehole at Dye 3 in Greenland. As explained in Chapter 11, northern-hemisphere ice deposited during the last ice age, when deformed in simple shear, has a value of A about 2.5 times that of ice deposited in the Holocene. The values in Table 5.1 refer to Holocene ice only. The value of Jezek and others is based on measured spreading rates of the Ross Ice Shelf but analyzed in a way different from that used by Thomas. Jezek and others deduced the stress resulting from the drag of grounded parts of the shelf, which tends to reduce the spreading rate, from the height of crevasses in the underside of the shelf. These heights were measured by radar.

TABLE 5.1. Measured values of flow parameter A at different temperatures for $n = 3$

T (°C)	A ($10^{-16}\,s^{-1}\,(kPa)^{-3}$)	Method	Reference
0	93	various lab tests	Budd and Jacka, 1989
	57	tilting of 5 boreholes	Raymond, 1980
	55	closure of 2 tunnels	Nye, 1953
	68	mean	
− 2	37	lab test	Steinemann, 1958a,b
	17	lab test	Barnes and others, 1971
	13	lab test	Morgan, 1991
	27	various lab tests	Budd and Jacka, 1989
	24	mean	
−10	3.0	lab test	Shoji and Langway, 1987
	3.5	various lab tests	Budd and Jacka, 1989
	8.7	borehole tilting	Dahl-Jensen and Gundestrup, 1987
	(0.57)	borehole closure	Paterson, 1977
	5.3	spreading of 5 ice shelves	Thomas, 1973b
	3.9	ice-shelf spreading	Jezek and others, 1985
	4.9	mean	

Borehole tilting and ice-shelf spreading measure tertiary creep, although not necessarily a steady-state value. Most of the laboratory tests

measured the minimum (secondary) creep rate. In some cases, however, the ice crystals had a preferred orientation that favoured deformation under the applied stress. Whether the amount of water in the ice used in the laboratory tests at 0°C was comparable with that in temperate glaciers is not known. These factors, and experimental inaccuracies, can easily explain the scatter in the values of A. The value derived from borehole closure is an exception. It is certainly the minimum creep rate but why it is so low is unclear. I have excluded it from the average.

My mean value $A = 4.9 \times 10^{-16}\,\mathrm{s}^{-1}\,(\mathrm{kPa})^{-3}$ at −10°C compares well with values of 4.5 and 5.0 in the same units derived from data compilations by Weertman (1983) and Hooke and Hanson (1986). My mean value for 0°C is the same as that derived from Eq. 4 for a water content of 0.625 per cent. This is within the range of water contents measured in a temperate glacier (Duval, 1977).

TABLE 5.2. Recommended values of flow parameter A at different temperatures and $n = 3$

T (°C)	A ($\mathrm{s}^{-1}\,(\mathrm{kPa})^{-3}$)
0	6.8×10^{-15}
− 2	2.4
− 5	1.6
−10	4.9×10^{-16}
−15	2.9
−20	1.7
−25	9.4×10^{-17}
−30	5.1
−35	2.7
−40	1.4
−45	7.3×10^{-18}
−50	3.6

Table 5.2 lists my recommended values of A. Those for 0°C, −2°C and −10°C are the mean values in Table 5.1. Other values are derived from that for −10°C by using the appropriate value of activation energy. If the water content of ice at melting point is known, the value derived from Eq. 4 is preferable to that in the table. If the ice has a strong single-maximum fabric that favours deformation in shear, as in ice-age ice in the northern hemisphere, it would be appropriate to use values of A about

2.5 times those in the table. This "enhancement factor" is obtained from field data (Paterson, 1991, Table 1).

PERFECT PLASTICITY

Instead of using the true flow relation, an approximation that is sometimes useful is to assume that ice behaves as a *perfectly plastic* material. Such a material does not start to deform until the stress reaches a critical value called the *yield stress.* At this point the strain rate becomes very large. This corresponds to letting $n \to \infty$. For, if we write $A = C\tau_0^{-n}$, Eq. 1 becomes

$$\dot{\epsilon}_{xy} = C(\tau/\tau_0)^n . \tag{23}$$

If $n \to \infty$,

$$\begin{aligned} \dot{\epsilon}_{xy} &\to 0 \qquad & \tau < \tau_0 \\ \dot{\epsilon}_{xy} &\to \infty \qquad & \tau > \tau_0. \end{aligned} \tag{24}$$

This corresponds to perfect plasticity with a yield stress of τ_0. The various flow relations are compared in Fig. 5.6.

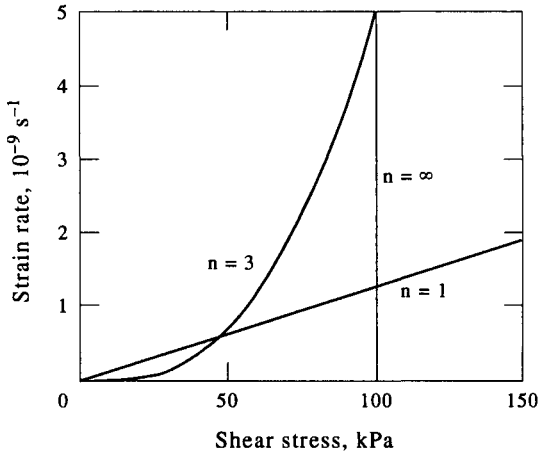

FIG. 5.6. Different types of flow relation: (a) Perfect plasticity with yield stress of 100 kPa, (b) Power law with $n = 3$, $A = 5 \times 10^{-15}$ s^{-1} (kPa)$^{-3}$, (c) Newtonian viscous flow with viscosity 8×10^{13} Pa s.

ANISOTROPIC ICE

The most extensive series of mechanical tests on anisotropic ice are those of Shoji and Langway (1988) on core from the 2037-m borehole through the Greenland Ice Sheet at Dye 3. The stress was uniaxial compression applied in different directions relative to the axis of the strong single-maximum fabric. Compression at 45° corresponds to simple shear parallel to the basal plane. The tests were made at constant strain rate $\dot{\epsilon}$ and so the stress varied with time. The important quantity is the maximum stress σ, which corresponds to secondary creep. No minimum was obtained in the test at 45° because this stress system is consistent with the existing fabric. All tests were made at −12.5°C .

Figure 5.7 shows the results for ice from a depth of 2006 m. The ordinate $\dot{\epsilon}/\sigma^3$ is $2A/9$ where A is the flow parameter (Eq. 17). For isotropic ice, I used the value obtained in tests on samples from a depth of 268 m where the ice crystals have random orientation. These data can be conveniently discussed in terms of the *enhancement factor*, the ratio of the measured strain rate to that of isotropic ice at the same stress and temperature.

The ice from 2006 m, which should be typical of deep ice from many parts of the polar ice sheets, is strongly anisotropic. For shear parallel to the basal plane, the enhancement factor is 19. At the other extreme, the enhancement factor for compression along the fabric axis, that is, perpendicular to the basal plane, is only 0.055; for compression perpendicular to the fabric axis it is 0.2. The strain rates in the most favourable and unfavourable directions thus differ by a factor of 345. For comparison, ice from a depth of 1890 m had enhancement factors of 9 for shear, 0.07 for compression along the fabric axis, and 0.5 for compression perpendicular to it. Duval and LeGac (1982) measured factors of 12.5 in shear and 0.25 in compression perpendicular to fabric axis in a sample from Law Dome, Antarctica. The scatter in these data must arise largely from differences in fabric strength although experimental inaccuracies may contribute.

To include the effect of anisotropy in analyses of glacier flow, the flow relation must be generalized. Johnson (1977) proposed such a generalization for an anisotropic material with an axis of symmetry. Such a material is isotropic in the plane perpendicular to this axis. Ice with a single-maximum fabric has this property. As before, the flow relation is assumed to depend only on stress deviators, not stresses, and to include only the second, not the third, invariant of the stress-deviator tensor. Johnson showed that, in this case, the flow relation can be expressed in terms of three parameters λ, μ, and ν and the index n. He derived equations relating strain-rate and stress components. The physical interpretation of the

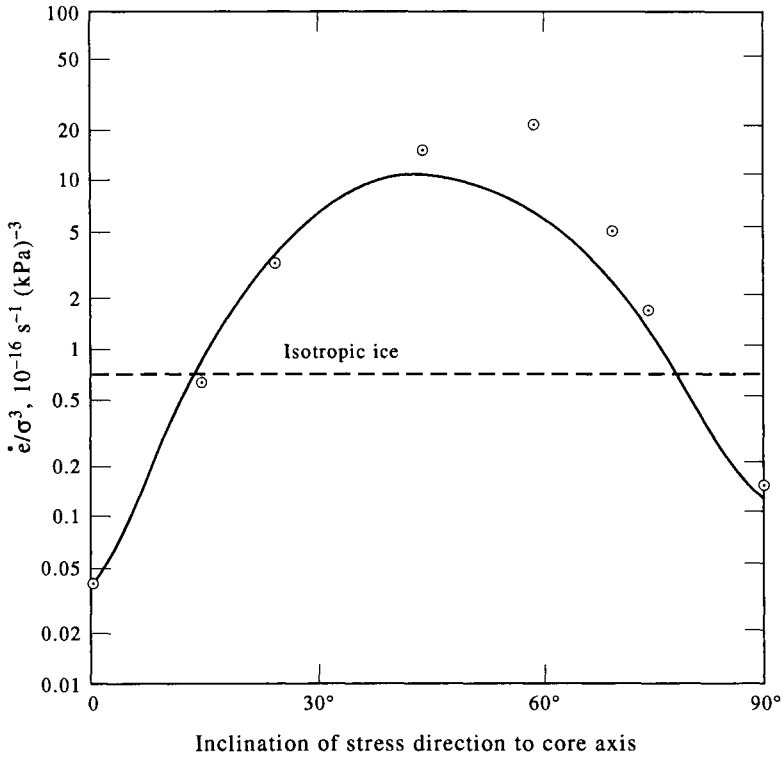

FIG. 5.7. Variation of $\dot{\epsilon}/\sigma^3$ (deformation rate divided by the cube of the stress) for ice with a strong single-maximum fabric deformed in uniaxial compression applied at different angles to the axis of the sample. The sample axis was within a few degrees of the fabric axis. Data from Shoji and Langway (1988). The curve is the variation predicted by the model of Johnson (1977).

parameters is made clear by considering special cases of these equations. If z is the axis of symmetry, and $n = 3$, for unconfined uniaxial compression σ_z, the equation for the strain-rate component reduces to $\dot{\epsilon}_z = \lambda^2 \sigma_z^3$ and so

$$\lambda^2 = \dot{\epsilon}_z / \sigma_z^3. \tag{25}$$

Similarly, uniaxial compression in any transverse direction gives

$$\mu^2 = \dot{\epsilon}_x/\sigma_x^3 . \tag{26}$$

Simple shear in the xz-plane gives

$$\nu^2 = 2\dot{\epsilon}_{xz}/\tau_{xz}^3 . \tag{27}$$

Comparison with Eqs. 16 and 17 shows that for isotropic ice

$$9\lambda^2 = 9\mu^2 = \nu^2 = 2A. \tag{28}$$

To fit this model to Shoji and Langway's data, take the z-axis in the direction of the fabric axis. The x-axis then corresponds to an inclination $\theta = 90°$. The values of λ and μ are then calculated from Eqs. 25 and 26. The value of ν can be calculated from measurements at one other value, say 45°, or at more than one and taking an average. The values, in units of $10^{-9}\,\mathrm{s}^{-1/2}\,(\mathrm{kPa})^{-3/2}$ are $\lambda = 2.0$, $\mu = 3.8$, $\nu = 148$. The strain rates corresponding to a given uniaxial stress at other inclinations θ can then be calculated from Johnson's equations. Figure 5.7 shows that the resulting curve is a reasonable fit to the data. There are sufficient data to calculate the values of the parameters at one other depth, 1890 m. They are $\lambda = 2.3$, $\mu = 5.9$, $\nu = 100$ in the same units.

For the case of a shear τ_{xz} combined with a compression σ_z, Johnson's equation for the shear strain rate reduces to

$$\dot{\epsilon}_{xz} = \tfrac{1}{2}\nu\,(\lambda\sigma_z^2 + \nu\tau_{xz}^2)\,\tau_{xz}. \tag{29}$$

With the above values of λ and ν, the weight assigned to the shear stress is 50 to 75 times that assigned to the compressive stress. Contrast this with the case of isotropic ice (Eqs. 19 and 21)

$$\dot{\epsilon}_{xz} = A\,(\tfrac{1}{3}\sigma_z^2 + \tau_{xz}^2)\,\tau_{xz}, \tag{30}$$

for which the ratio is only 3. Thus, because the fabric makes the ice soft for shear but hard for compression, the effect of the compressive stress on the shear strain rate is greatly reduced.

In contrast to the above, Lliboutry and Andermann (1982) concluded, from data less extensive than Shoji and Langway's, that Johnson's equations were inadequate to describe the deformation of ice with a single maximum fabric. They proposed a relation with six parameters only three of which could be determined from the data. Pimienta and others (1987) analyzed the results of mechanical tests on ice from Vostok, Antarctica,

which has a girdle fabric, in terms of the same relation. Again only three parameters were determined from the data; the others were estimated from a theoretical model with additional assumptions.

There appear to be no data on the deformation of ice with a fabric with several maxima as found in the basal layers of polar ice sheets at places, such as Byrd Station, Antarctica, where the temperature is greater than about −10°C. Lliboutry and Duval (1985) state that this ice can be regarded as isotropic.

Most of the ice in glaciers and ice sheets has a non-random crystal orientation. This is ignored in nearly all theoretical analyses of glacier flow. There is an urgent need for more data for testing the adequacy of proposed anisotropic flow relations such as those of Johnson (1977) and Lliboutry (1983b). An added complication is that crystal fabric develops slowly. Thus, provided that the stress system remains the same, the fabric strength and the anisotropy increase with increasing total strain, at least up to a limiting value. A flow relation for ice-sheet modelling should take account of this.

FURTHER READING

The book by Hobbs (1974, p. 18–24) contains further details of the structure of ice. Weertman (1983) discusses the creep properties of ice as derived from both laboratory and field studies. Hobbs (1974, Chapter 4) and Glen (1975) have reviewed the mechanical properties of ice, elasticity and fracture as well as creep, and Mellor (1975) the mechanical properties of snow and firn.

The existence of ice caps on Mars, and the discovery that some of the moons of Jupiter and Saturn consist largely of ice, have stimulated laboratory studies of the rheology of ice and ice-silicate mixtures at low temperatures and high pressures. Papers by Poirier (1982) and Kirby and others (1985) provide an introduction to this work.